Journal of Atmospheric and Solar-Terrestrial Physics 72 (2010) 334–343

Contents lists available at ScienceDirect

Journal of Atmospheric and Solar-Terrestrial Physics

journal homepage: www.elsevier.com/locate/jastp

The November 2004 superstorm: Comparison of low-latitude TEC observations with LLIONS model results

Matthew A. Hei *, Cesar E. Valladares

Boston College, Institute for Scientific Research, St. Clement's Hall 412, 140 Commonwealth Avenue, Chestnut Hill, MA 02467-3800, USA

ARTICLE INFO

Article history:
Accepted 25 March 2009
Available online 7 April 2009

Keywords:
EIA
CPZ
Superstorm
Superfountain
GPS
TEC

ABSTRACT

We investigate the effects of penetration electric fields, meridional thermospheric neutral winds, and composition perturbation zones (CPZs) on the distribution of low-latitude plasma during the 7–11 November 2004 geomagnetic superstorm. The impact on low-latitude plasma was assessed using total electron content (TEC) measurements from a latitudinally distributed array of ground-based GPS receivers in South America. Jicamarca Radio Observatory incoherent scatter radar measurements of vertical $\mathbf{E}\times\mathbf{B}$ drift are used in combination with the Low-Latitude IONospheric Sector (LLIONS) model to examine how penetration electric fields and meridional neutral winds shape low-latitude TEC. It is found that superfountain conditions pertain between ~1900 and 2100 UT on 9 November, creating enhanced equatorial ionization anomaly (EIA) crests at $\pm 20^{\circ}$ geomagnetic latitude. Large-amplitude and/or long-duration changes in the electric field were found to produce significant changes in EIA plasma density and latitudinal location, with a delay time of ~2–2.5 h. Superfountain drifts were primarily responsible for EIA TEC levels; meridional winds were needed only to create hemispherical crest TEC asymmetries. The $[O/N_2]$ density ratio (derived from the GUVI instrument, flown on the TIMED satellite) and measurements of total atmospheric density (from the GRACE satellites), combined with TEC measurements, yield information regarding a likely CPZ that appeared on 10 November, suppressing TEC for over 16 h.

1. Introduction

Geomagnetic storms have long been known to cause strong effects at high latitudes. Particle precipitation in this region ionizes neutral particles, heats the thermosphere, and excites outer shell electrons of some neutral particles into higher energy levels. Consequently, thermospheric heating alters neutral wind patterns, and relaxation of excited electrons to lower energy levels releases energy in the optical range; these emissions are known as the aurora. Furthermore, electric fields also map to low altitudes here from the magnetosphere, driving ionospheric convection cells and joule heating.

In recent years, it has become increasingly apparent that storms play an important role in mid- and low-latitude ionospheric plasma dynamics. Electric fields are one means by which high-latitude processes couple to lower latitudes. Both prompt penetration electric (PPE) fields (Fejer et al., 1979, 1990; Fejer and Scherliess, 1995; Kelley et al., 1979) and disturbance dynamo (DD) generated electric fields (Blanc and Richmond, 1980; Fejer and Scherliess, 1995; Richmond et al., 2003) at times map all the way to the geomagnetic equator. These fields in turn alter the existing seasonal and diurnal plasma $\mathbf{E}\times\mathbf{B}$ drifts, thereby redistributing plasma, most significantly in latitude and altitude. In particular, electric fields that penetrate to low latitudes may add vectorially to existing dynamo-generated zonal electric field to either reinforce or suppress what is known as the fountain effect. In the fountain effect (Kelley, 1989), an Eastward electric field, combined with the nearly horizontal geomagnetic field at very low latitudes (approximately $\pm 5^{\circ}$ geomagnetic latitude), will cause ionospheric plasma to $\mathbf{E}\times\mathbf{B}$ drift vertically upwards. Subsequently, gravity and pressure gradients cause the plasma to drift down along magnetic field lines to higher latitudes, resulting in two regions of enhanced plasma density together known as the equatorial ionization anomaly (EIA), or simply the "equatorial anomaly". For historical reasons, the EIA is also known as the Appleton anomaly. When strong PPE or DD electric fields reinforce the nominal daytime Eastward field, plasma is driven to very high altitudes. Magnetic field lines at higher altitudes have footpoints at higher latitudes; thus, ionization crests form at higher latitudes. During strong storms, when the Eastward field is substantially reinforced, the phenomenon is known as the "superfountain effect" (Tsurutani et al., 2007). It also sometimes

* Corresponding author. Now at Naval Research Laboratory, Plasma Physics Division, Code 6754, 4555 Overlook Ave, SW Washington, DC 20375, USA. Tel.: +1 202 767 3828; fax: +1 202 767 0631.
E-mail addresses: hei@ppd.nrl.navy.mil (M.A. Hei), valladar@bc.edu (C.E. Valladares).

1364-6826/$ - see front matter © 2009 Elsevier Ltd. All rights reserved.
doi:10.1016/j.jastp.2009.03.025

happens that a Westward electric field penetrates to low latitudes and suppresses the fountain effect. In this case, the EIA crests move to correspondingly lower latitudes. PPE electric fields typically affect the low-latitude plasma distribution in a symmetric manner. However, DD electric fields, meridional neutral winds, and other effects may introduce TEC asymmetries between hemispheres.

Meridional neutral winds may induce asymmetries in the low-latitude total electron content (TEC) distribution in two ways. First, through ion-neutral collisional processes, they directly change the transport of plasma parallel to the magnetic field. This effect dominates at higher altitudes near the geomagnetic equator, where the dip angle is small and a horizontal meridional wind acts essentially parallel to the geomagnetic field. A northward wind will thus act to push plasma along field lines to the leeward/Northern Hemisphere, resulting in an enhanced northern anomaly crest. While it is true that plasma on the southern arc of the equatorial fountain will have a horizontal velocity component in the southern direction, acting in opposition to a northward wind, its horizontal velocity component is small relative to the vertical fountain drift, especially at higher altitudes. Thus, a meridional neutral wind of the order of tens of m/s will overwhelm this flow and redistribute plasma to the leeward hemisphere. Second, again through ion-neutral collisional processes, meridional winds drive plasma up along magnetic field lines on the windward side and down field lines on the leeward side (Hargreaves, 1992). This effect dominates at lower altitudes near the footpoints of geomagnetic field lines, where the angle between the horizontal wind vector and the field lines is significant (i.e., dip angle $>20^{\circ}$). Because recombination reactions are proportional to concentration (i.e., inversely proportional to altitude), the leeward side will experience a faster loss of ionization relative to the windward side, creating a TEC deficit in the leeward hemisphere. This effect is most important during the evening and night, when solar ionization and interhemispheric transport effects weaken or cease entirely. Conversely, as will be seen in the LLIONS (Low-Latitude IONospheric Sector) model results, interhemispheric transport of plasma and solar ionization dominate loss processes during the day.

Equatorward wind surges are a mechanism by which high-latitude effects may propagate to low latitudes to create an asymmetric distribution of plasma across the geomagnetic equator. Particle precipitation and joule heating in the auroral region heat the thermosphere, which then rises and expands. Since these parcels of upwelling neutrals originate at relatively low altitudes, they are enriched with heavy neutrals compared with the background atmosphere. These parcels are then typically driven equatorward by some combination of storm winds and existing seasonal/diurnal meridional winds (Lin et al., 2005a). Due to their enriched heavy neutral content, they are termed "composition perturbation zones", or CPZs. Under the right conditions, CPZs may reach low latitudes – even the geomagnetic equator – where they can significantly alter the local recombination chemistry. Molecular Nitrogen, in particular, will accelerate loss reactions, rapidly quenching the local plasma density. A hemispherical asymmetry in the background/stormtime wind magnitude, CPZ maximum latitudinal penetration, or CPZ chemical composition/concentration will induce a corresponding asymmetry in the low-latitude TEC, provided that a CPZ reaches the latitude of at least one anomaly crest.

Until recently, it has been very difficult to measure all of the effects thus described. The large distances involved, lack of distributed instrumentation, and relative rarity of storms all have contributed to this problem. However, in recent years large-scale deployment of GPS receivers has proceeded rapidly throughout the South American sector. These distributed arrays make it possible to make maps of total electron content covering wide geographic areas. When supplemented by computer models, GPS receiver TEC measurements have been shown to be a powerful tool for mapping the three-dimensional distribution of plasma at low latitudes (Lin et al., 2005a, b; Valladares and Sheehan, 2001; Valladares et al., 2004). Early studies show that CPZs and penetration electric fields (Lin et al., 2005a, b), as well as seasonal/diurnal meridional neutral wind patterns (Valladares and Sheehan, 2001; Valladares et al., 2004), strongly influence low-latitude plasma dynamics and chemistry.

The November 2004 superstorm represents a unique opportunity to study stormtime effects. Never before have such a wide array of instruments simultaneously observed a storm of this magnitude (Kelley et al., 2009). Most significantly, this is the first time that continuous measurements of the vertical plasma drift near the geomagnetic equator have been available during a large portion of a superstorm. Previously, the best superstorm vertical drift data available were from the ROCSAT-1 satellite, for the October–November 2003 superstorm (Lin et al., 2005b). Jicamarca Radio Observatory (JRO) drift data offer improved accuracy, without the limitations imposed by satellite orbital motion and the precession of the satellite orbit. By continuously measuring the vertical plasma velocity in a single geographic sector, JRO data thus make it possible to separate out effects due to stormtime penetration electric fields from the complex array of stormtime and background drivers of the low-latitude plasma distribution.

In this work, we use TEC data from the South American array of GPS receivers, combined with Jicamarca vertical drifts to study the impact of stormtime penetration electric fields on the low-latitude plasma distribution. Additionally, we utilize other data sets to ascertain the impact of CPZs and LSTIDs. To determine the role of meridional neutral winds, we drive the Low-Latitude IONospheric Sector model with the Jicamarca vertical drift data. In this way, we determine the relative roles of the various drivers under superstorm conditions.

2. Instrumentation and data sets

Measurements of TEC were made using an array of 12 GPS receivers located in South America (Valladares et al., 2004). The receivers are situated between 70° and 80° W longitude, and span the latitude range of 9° N–40° S. Receiver locations are depicted in Fig. 1. Raw slant-TEC (STEC) measurements were converted into vertical (VTEC) values to remove TEC perturbations due to raypath length. Plots of VTEC versus geographic latitude and local time were then made by performing a two-dimensional regression analysis of the TEC values. An example of such a plot is shown in Fig. 2.

Plasma vertical drift velocities at the equator were provided by the Jicamarca incoherent scatter radar (ISR), operating in drift mode (Kudeki et al., 1999). The radar measures the plasma velocity between the altitudes of approximately 150–900 km with a 15-km vertical resolution and 5-min sample rate. F-region line-of-sight uncertainties in the drift are less than 1.0 m/s, even under the low signal-to-noise ratio conditions (SNR ≈ 0.1) typically seen away from the F-region density peak (Kudeki et al., 1999). Continuous ISR data are available from 12 UT on 9 November up through to the beginning of 11 November 2004. For the present work, the rise velocity at the geomagnetic equator was taken to be the average of the Jicamarca ISR rise velocity between 200 and 400 km altitude.

Data from the Global Ultraviolet Imager (GUVI) on the Thermosphere Ionosphere Mesosphere Energy and Dynamics (TIMED) satellite were used to examine the $[O/N_2]$ density ratio as a function of latitude, longitude, and local time. A reduced $[O/N_2]$ ratio indicates the presence of a molecular-enriched CPZ,

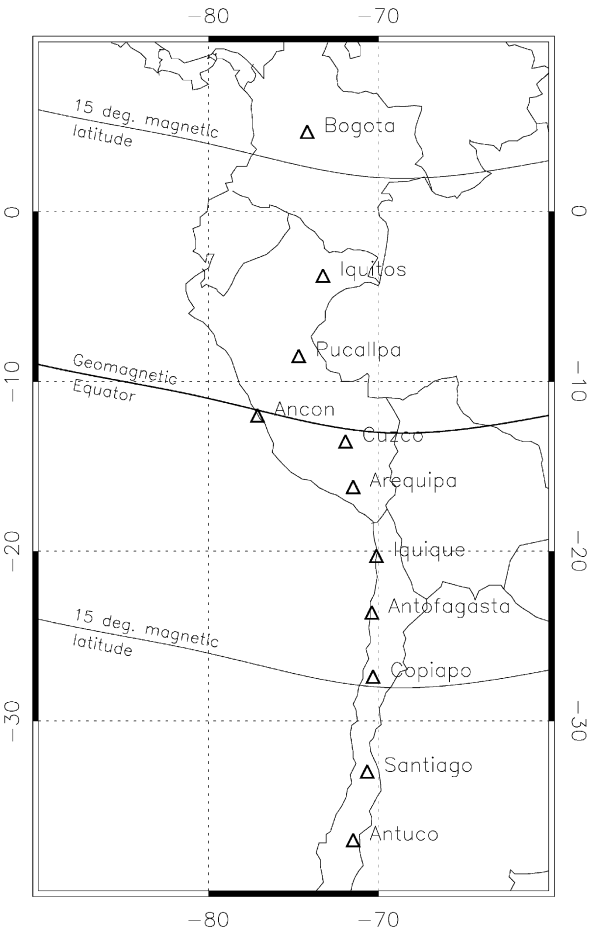

Fig. 1. The South American array of GPS receivers.

where recombination reactions are expected to proceed at an accelerated rate. GUVI is a far-ultraviolet scanning imaging spectrograph. This instrument performs limb and disk scans in five wavelength intervals: HI (121.6 nm), OI (130.4 nm), OI (135.6 nm), and the N_2 Lyman–Birge–Hopfield bands LBH_S (140–150 nm) and LBH_L (165–180 nm). Strickland et al. (1995) discovered a linear relationship between the $[O/N_2]$ ratio and the ratio of the 135.6/LBH_S frequency bands. The data used in this study were processed using the techniques of Strickland et al. (2004) and Zhang et al. (2004) to obtain $[O/N_2]$, the thermospheric column number density ratio of O and N_2, referenced to an N_2 column number density of 10^{17} cm^{-2}. The TIMED satellite has a 630-km, 74.1° inclination circular orbit; its orbital period is 97.8 min.

Measurements of total atmospheric density were provided by the Spatial Triaxial Accelerometer for Research (STAR) sensors on the Gravity Recovery and Climate Experiment (GRACE) satellites. GRACE consists of two satellites flying in tandem in a near-circular, polar orbit at an approximate altitude of 485 km; the satellites are separated by ~220 km. The STAR instruments measure nongravitational forces on the satellite (Bruinsma et al., 2004; Bruinsma and Biancale, 2003), from which estimates of atmospheric neutral density are derived.

3. The LLIONS model

TEC measurements are compared to TEC distributions derived from the Low-Latitude IONospheric Sector model. LLIONS is a physics-based numerical model of the E- and F-region ionosphere that has its origins in the low-latitude ionosphere model (LowLat) (Anderson, 1973, 1981). Subsequently, LowLat was incorporated into a global ionospheric model called the Ionospheric Forecast Model (IFM) (Schunk and Sojka, 1997); LLIONS is a version of IFM optimized to produce meridional slices of the low-latitude ion

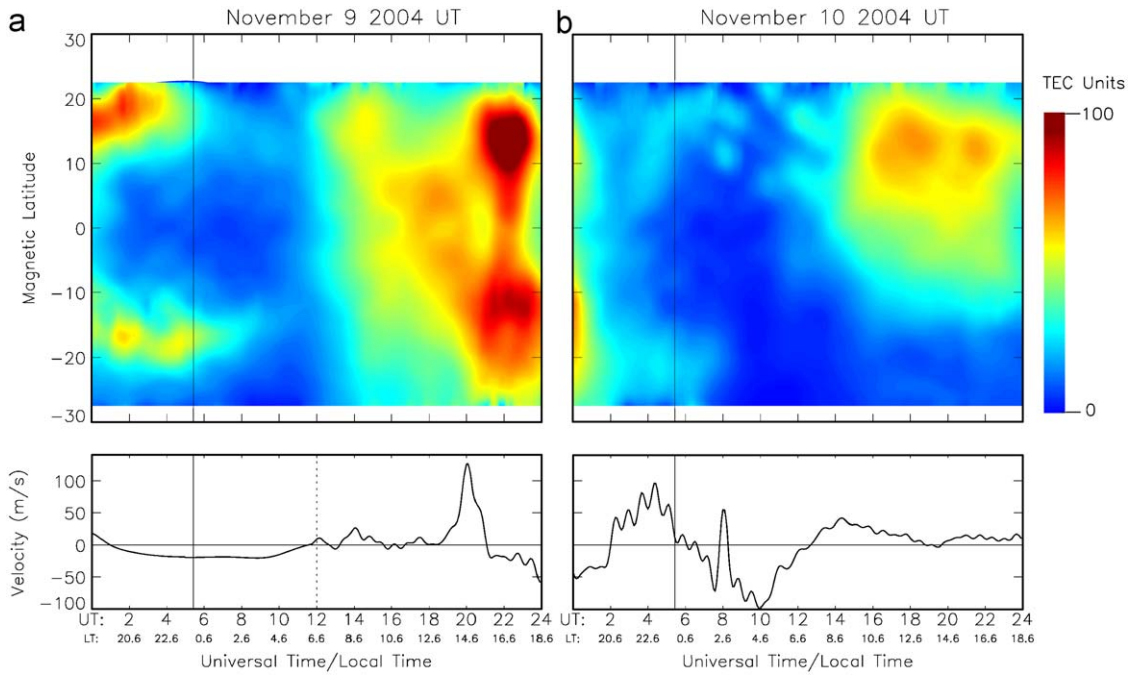

Fig. 2. Observed TEC (South American Array of GPS receivers) for (a) 9 November and (b) 10 November, 2004. VTEC is plotted in the top panels, Jicamarca vertical drift velocity is plotted in lower panels. Note that Jicamarca drift data begins at 1200 UT on 9 November; previous to this Fejer-Sherliess climatological values are presented; a dotted vertical line separates measured drift values from climatological values. Vertical solid lines in all plots demarcate local time midnight.

density distributions (Anderson et al., 2006). In recent years, Vince Eccles has made numerous upgrades and refinements of the LLIONS model (Eccles et al., 2004).

LLIONS calculates the two-dimensional, time-dependent density distributions of five major plasma constituents (NO^+, O_2^+, H^+, O^+, e^-) between $\pm 40^\circ$ latitude and 90–4000 km altitude, with a spatial resolution of 4 km in the E-region and 20 km in the F-region. Three-dimensional global distributions are obtained through multiple runs of the code. Additional outputs include global specifications of VTEC, N_mF_2, and h_mF_2. Inputs to the model include vertical $\mathbf{E} \times \mathbf{B}$ drift velocities at the geomagnetic equator, zonal and meridional neutral winds, neutral atmospheric densities and temperatures, the Kp index and $F_{10.7}$ cm flux, and the rates of ionization production, loss, and diffusion.

4. Observations

The basic characteristics of the November 2004 superstorm and the instruments employed for observations are described in Kelley et al. (2009); here we focus on the aspects of the storm and observations pertaining to the low-latitude region. It should be noted that while this paper focuses on data acquired on the 9th and the 10th, the initial phase of the superstorm actually occurred on the evening of the 6th. Subsequently, the first main phase occurred between midnight and noon on 7 November; the DST index reached its first minimum of −400 NT at approximately 0600 UT that day. After recovering to −100 NT on the 8th, the DST reached a second minimum of −300 NT on the 10th, with the second main phase occurring between roughly 2100 UT on 9 November and 2300 UT on 10 November. Thus, it is possible that observations on the 9th and 10th are a convolution of penetration field, disturbance dynamo, and nominal background dynamo electric fields.

Examination of Jicamarca Radio Observatory ISR vertical drifts does indeed reveal a low-amplitude, high-frequency component that is likely due to disturbance dynamo fields originating from the first main phase of the superstorm. However, these effects are minor in comparison to the effect of the penetration electric fields, which overwhelm both DD and seasonal/diurnal dynamo fields over short ($\leqslant$2-h) timescales. Kelley et al. (2009) found an 85% correlation between IEFy and JRO E-fields during the period 10–21 UT on the 9th, a period that included the 120 m/s rise of the F-layer (19–21 UT). Kelley also found a period of anticorrelation of longer duration (05–13 UT on the 10th); they conclude that the reversal in the plasma velocity during this time is the result of a local time dependence of the PPE effect. Thus, JRO drift velocity data show that penetration fields are the dominant driver of the low-latitude plasma vertical velocity during much of the period under consideration.

Contours of TEC from the South American array are plotted as a function of UT and latitude in Fig. 2. Data from 9 November (UT) are presented in Fig. 2a, and data from 10 November are shown in Fig. 2b; below each contour plot is the vertical rise velocity as measured at Jicamarca (Jicamarca measurements begin at 1200 UT on 9 November; velocity values before this time are from the Fejer–Sherliess drift model (Scherliess and Fejer, 1999). The solid vertical line in all panels denotes local midnight, while the dotted vertical line in the 9 November velocity plot demarcates the beginning of the JRO measurements. Discussion of observations will be limited to times when Jicamarca drifts were available.

Three features are most evident in the 9 November contours. First is the dramatic increase in TEC beginning at approximately 1200 UT on the 9th (sunrise) and continuing until reaching a maximum at 2230 UT. The slow steady increase at all latitudes during this period is primarily due to the action of solar ionization, whereas the rapid increase seen at $\pm 20^\circ$ geomagnetic latitude is due to the superfountain effect. The Jicamarca drift data show that there is a roughly 2.5-h delay between the peak upward drifts centered on 2000 UT and the maximum Appleton peak densities seen at 2230 UT. Second, the peak ionization level at 2230 UT is higher in the northern crest (124 TEC units) than in the southern crest (97 TEC units). Somewhat higher northern crest TEC levels are expected at this longitude in November. The offset between the geomagnetic and geographic equators at this time ensures that the subsolar point is closer to the latitude of the northern crest, leading to more intense and longer periods of ionizing sunlight in the northern crest region. However, LLIONS model results, discussed in the next section, show that a northward meridional thermospheric wind likely contributes significantly to this latitudinal TEC asymmetry. Third, while TEC decreases rapidly at all latitudes during the evening, the northern peak decays at a much faster rate than the southern peak. Indeed, the northern peak decays so fast that, for a brief period near 2400 UT (18.6 LT), northern crest TEC is much lower than southern crest TEC—a somewhat surprising reversal. The rapid TEC decay seen at all latitudes is primarily due to decreased photoionization near sunset (~2400 UT) combined with strong downward drifts between 2200 UT on 9 November and 0200 UT on 10 November; the downward drifts take the plasma into a region of higher neutral concentration (and correspondingly faster recombination rates). LLIONS model results suggest that the latitudinal asymmetry in crest TEC decay is caused, at least in part, by a northward thermospheric wind.

Fig. 2b shows the TEC distribution for 10 November. TEC continues to decay rapidly at all latitudes during the (local time) evening hours. The northern crest TEC remains lower than the southern during the entire decay period up until approximately 0600 UT, when the crest TEC levels are approximately equal. During the period 0200–0700 UT, TEC levels are sustained at $\pm 20^\circ$ due to strong upward plasma motion at the equator. Beginning at 0800 UT, the southern-sector TEC is rapidly quenched, reaching almost negligible levels by 1000 UT. TEC levels remain suppressed in the South even after sunrise (~1200 UT), when photoionization reestablishes the northern crest at nearly typical nonstorm levels. Note that the magnitude of the N–S asymmetry is much greater than it was on the 9th during the same LT interval. Two possible causes for the sudden and persistent suppression of plasma density in the South include a CPZ that reduced the southern sector [O/N_2] ratio, or a reversal of the meridional neutral wind. In the early evening (2200–2400 UT), the northern peak decays quickly, though not as sharply as the preceding day. A slower decay rate could be the result of either a weakened (or a reversed) northward wind or a lower ion concentration relative to the peak on the 9th.

It is clear from Fig. 2 that while much of the latitudinal variation of TEC is due to the vertical drift near the geomagnetic equator, CPZs, meridional neutral winds, and other effects also appear to play a significant role. Other data sets and the LLIONS model are useful for determining the relative roles of these other drivers. We first describe in this section the observations; LLIONS results are presented in the next section.

(Lin et al., 2005b) demonstrated that the GUVI-derived [O/N_2] ratio may be used to trace stormtime CPZ activity, despite limitations in local time and longitude coverage imposed by the satellite orbit. Lower [O/N_2] ratios indicate the presence of CPZs, and hence presumably faster recombination. Thus, it is expected that areas of significantly suppressed [O/N_2] ratio will correspond to areas of reduced TEC. Fig. 3 depicts [O/N_2] ratio data from multiple GUVI orbits for 9 November and 10 November. Throughout the low-latitude South American sector on the 9th,

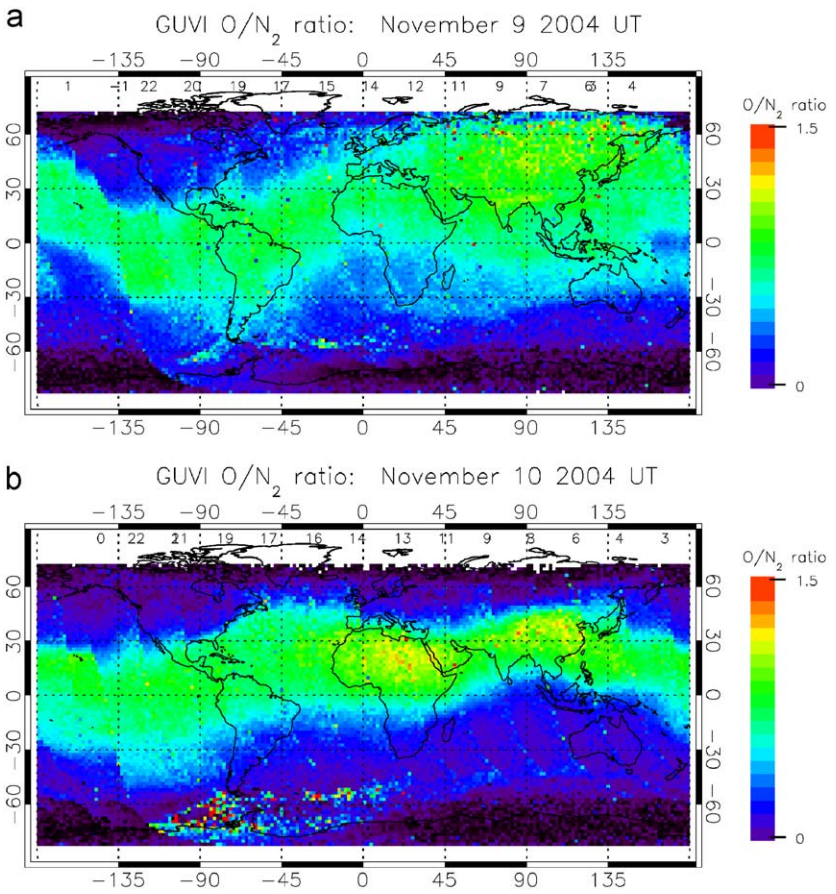

Fig. 3. GUVI [O/N_2] ratio on (a) 9 November and (b) 10 November. The approximate time the satellite crossed the equator during each orbit is plotted at the corresponding approximate longitude at the top of the plot.

a moderate [O/N_2] ratio pertains. In contrast, on the 10th at ~1900 UT (1500 LT in the American sector) a substantial latitudinal gradient exists, with the Northern Hemisphere retaining [O/N_2] values comparable to those seen on the 9th, and the Southern Hemisphere [O/N_2] ratio falling to much-reduced levels. Given the restrictions imposed on the data by the satellite orbit and field of view, it is not possible to determine for how long before and after 1900 UT this latitude gradient persists. However, 1900 UT is well within the period when the southern anomaly crest essentially disappears, revealing a clear correlation between suppressed TEC and reduced [O/N_2] ratio. Thus, the suppressed TEC from approximately 0800–2400 UT on 10 November appears to be due to a CPZ accelerating recombination in the southern crest region.

GRACE observations for this period indeed reveal an equatorward-propagating region of enhanced neutral density. Again, the satellite orbital cadence (typical LEO, i.e., ~100 min) imposes limitations, but the interval is short enough to see neutral density disturbances propagating from the poles towards the equator. Fig. 4 shows three orbits of GRACE neutral density data. Each panel/orbit is separated by approximately 90 min UT. Since GRACE is in a near-polar orbit (89.5°), there is minimal variation in local time within a given orbit. A surge in neutral density appears to progress equatorward from the Southern Hemisphere with increasing UT. The estimated longitude of the surge is marked by a vertical line. In the first panel (1.27 UT) the surge appears to be at −63°, whereas the surge appears to progress to −52° and then −41° in the second and third panels, respectively. This yields an approximate velocity of 230 m/s, placing it at 25° S (~10° S geomagnetic) at ~0900 UT (~0330 LT at Jicamarca). This timing corresponds very well with the sudden, rapid decay of the Southern Hemisphere TEC beginning at approximately 0800–1000 UT. Southern crest TEC remains severely depleted between this time until 1900 UT when the GUVI measurements were taken, suggesting that a neutral surge was indeed the causative mechanism.

IMF data, coupled with Northern-Hemisphere radar chain and ionosonde data, are consistent with 0900 UT on 9 November as a likely arrival time of a neutral surge. Strong auroral heating appears to have begun at approximately 1900 UT on 9 November, when the IMF turned southward, coupling the Earth's magnetic field with the solar wind magnetic field. At this time, the AE index rose to 1800 nT, a level indicative of strong auroral forcing, and frequently associated with the creation of LSTIDs. One hour later at 2000 UT the Millstone Hill ISR observed strong horizontal winds indicative of TIDs (Erickson and Goncharenko, 2009). A short time later at 2030 UT the Wallops Island (Virginia) Digisonde observed TID signatures; still later at 2100 UT TID signatures were seen by the Ramey Digisonde in Puerto Rico. The Arecibo ISR, also located in Puerto Rico (~18.3° geodetic latitude), provided an even better observation of the LSTIDs, though the radar was switched on for observations slightly after 2100 UT. Three pulses were observed at ~2100 UT (9 November), ~0400 UT (10 November), and ~1100 UT (10 November). Estimates of LSTID propagation velocity based on the timing of the Millstone Hill-Wallops Island observations yield ~310 m/s; Wallops Island-Arecibo observations give ~1300 m/s. By splitting the difference and assuming a propagation velocity of ~800 m/s (typical for LSTIDs), these disturbances should reach the low-latitude region (~10° N latitude) between approximately 2130 UT on 9 November

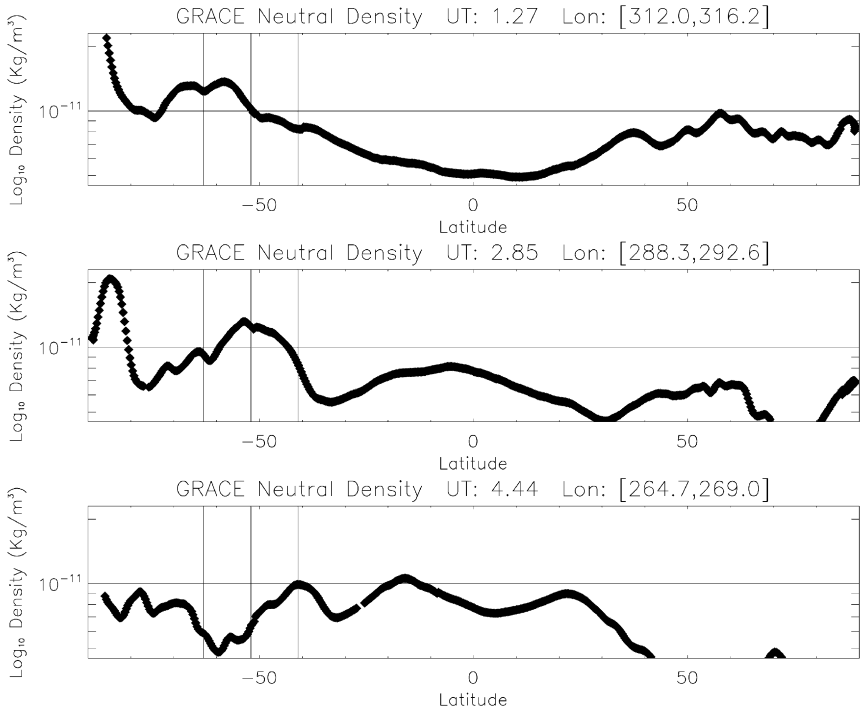

Fig. 4. Three partial orbits of GRACE neutral density data as a function of latitude for 10 November 2004 UT. At the top of each figure the UT at the center of the pass (~0° geographic latitude) and the longitude range (longitude of the satellite at ±50° geographic latitude) is given. Vertical lines trace the movement of the neutral surge. The first vertical line corresponds to the peak location in panel 1, the second vertical line corresponds to the peak location in panel 2, etc. The peak moves approximately 11° between panels 1 and 2 and again approximately 11° between panels 2 and 3.

and 1130 UT on 10 November. Thus, LSTID activity is present in the Northern-Hemisphere low-latitude region during the 11 h preceding, and for 2 h following the suspected arrival time of the CPZ on the 10th in the conjugate hemisphere. Combined with the apparent onset of auroral heating in the Northern Hemisphere at ~1900 UT on 9 November, this timing is consistent strong polar effects propagating to low latitudes during the estimated time of arrival of the CPZ.

5. LLIONS model results

The extensive observations of the 2004 Superstorm reveal a great deal about stormtime dynamics and chemistry. However, crucial gaps in our understanding still exist. Most significantly, thermospheric wind measurements were not made for this storm. In their absence, it is useful to model the neutral winds, in particular the meridional thermospheric neutral winds, and observe their impact on the low-latitude plasma distribution as seen in the calculated TEC. Our approach is to utilize JRO vertical drift measurements to drive the LLIONS model for the period under study. The effect of meridional neutral winds is studied by injecting winds of varying magnitude and sign into the simulation and observing the latitudinal asymmetries in calculated TEC that result. While it is possible to drive the model with a superposition of modeled winds (e.g., the Hedin Wind Model) added to a constant perturbation wind to simulate stormtime conditions, we opt instead to simply inject constant meridional wind values without relying on wind model results. Our approach makes it possible to isolate the role of the first-order neutral wind without complicating the analysis by introducing wind model-based assumptions or errors into the LLIONS results.

The ensemble of LLIONS model runs is created by driving LLIONS with meridional winds of varying magnitude and sign (for simplicity of interpretation, zonal and other winds are not included in this study). The winds are modeled in geographic coordinates, and are ranged between 125 m/s north and 125 m/s south in 25 m/s increments. By way of comparison, typical solstice winds are of the order of 25 m/s (Rishbeth et al., 2000). Again for simplicity of interpretation, wind velocities are held constant over all altitudes, latitudes, and local times for a given 3-day run (8–10 November 2004). Discrepancies between the data and model results can in part then be explained in terms of the wind magnitude being over or underestimated. Only the meridional neutral winds are varied across ensemble runs: all other drivers, inputs, and background conditions remain unchanged. High-resolution JRO drifts drive the model beginning at 1200 UT on 9 November. Prior to this, drifts from the Fejer–Sherliess model are used. Neutral atmospheric densities and temperatures are obtained from the MSIS-90 empirical model.

Fig. 5 compares TEC observations with LLIONS-derived TEC for 9 November and 10 November. In each panel, TEC is plotted as a function of geomagnetic latitude and time (UT and LT). Array TEC is presented in panel a; panels b, c, d, and e present LLIONS TEC with meridional winds of 100 m/s north, 50 m/s north, 0 m/s, and 50 m/s south, respectively. The lifting/lowering effect of the wind near fluxtube footpoints is most evident on 9 November between approximately 0400 and 1200 UT (panels b through e). In panel d, the plasma distribution is essentially symmetric about the geomagnetic equator. As the northward wind increases in panels c and b, however, TEC is seen to increase in the windward (southern) hemisphere between roughly −15° and −30°, whereas it decreases symmetrically in the 15–30° sector. Conversely, a TEC increase between 15° and 30° is seen in the same UT sector under southward wind conditions (panel e), with a corresponding TEC decrease in the −15° and −30° sector. It should be noted that the lifting effect is present at all times in all model runs with nonzero wind. Whereas this effect is clearly dominant between 0400 and 1200 UT on 9 November, it competes at other times with superfountain dynamics and high-altitude wind effects.

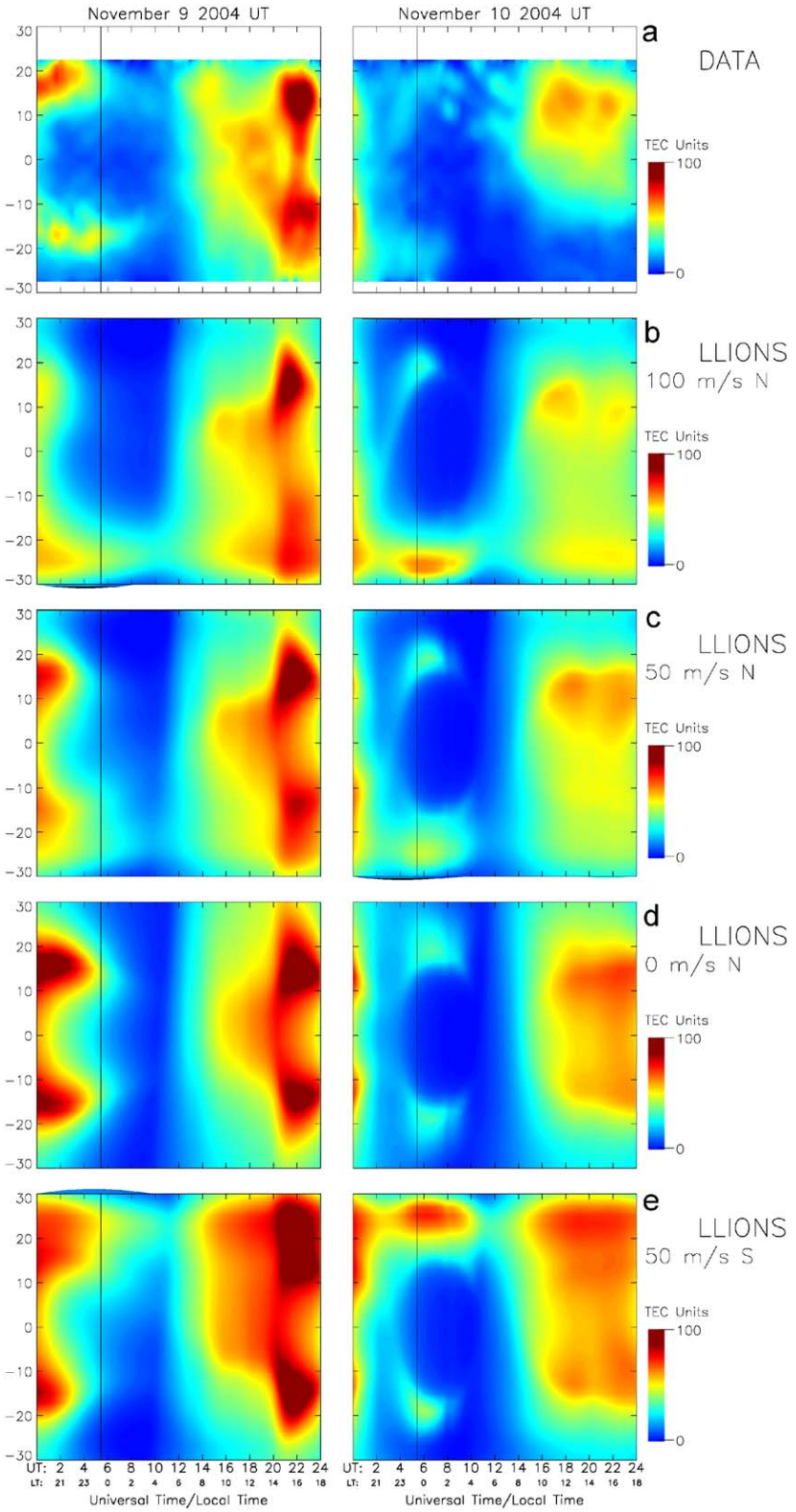

Fig. 5. (a) Observed TEC and (b–e) LLIONS-derived TEC with various input meridional wind speeds.

The effect of high-altitude winds on the low-latitude plasma distribution is also evident on the 9th, primarily between 2000 and 2400 UT, but also between 0000 and 0400 UT. During these times the strong zonal electric field at the geomagnetic equator lifts very dense plasma to high altitudes, where the zonal wind, through collisional processes, drives it along field lines from one hemisphere to another. The TEC asymmetry seen in panels b through d is consistent with this action of high-altitude winds. Anomaly crests show increasing asymmetry as the northward wind increases between panels d and b, with the northern crest becoming significantly more enhanced relative to the southern. It should be noted that even under no-wind conditions (panel d), the

northern crest is slightly enhanced relative to the southern. The closer proximity of the subsolar point to the northern crest is the likely cause of this enhancement. More specifically, the subsolar point is located between approximately 0° and −10° geographic latitude due to the season. However, the geomagnetic and geographic equators are offset by approximately 10° in the South American longitude sector. In geomagnetic coordinates the subsolar point is between 0° and 10° geomagnetic latitude, placing the subsolar point closer to the northern crest. The closer proximity of the subsolar point to the northern crest also appears to influence the TEC distribution during southward wind conditions (panel e). Noticeably higher TEC levels appear at the northern crest (given the higher levels and longer periods of ionizing solar radiation during the day); correspondingly higher TEC levels also appear in the southern crest, presumably due to the continual replenishment of plasma in the northern crest, which should then subsequently blow south to the opposite crest. Finally, in all cases where wind is present, the off-equator lifting/lowering effect is also evident between 2000 and 2400 UT. This effect causes the southern anomaly crest to become more extended in latitude, and the northern crest to be more restricted in latitude, as the magnitude of the northward wind increases.

The LLIONS TEC results are very different on the 10th; however the effects of meridional winds, solar ionization, and the plasma vertical drift velocity at the geomagnetic equator are easily seen. Most noticeably, in all cases of nonzero wind, the leeward anomaly crest TEC decays more rapidly in the early evening/postsunset hours (∼2300 UT on 9 November to 0300 UT on 10 November). This is an expected consequence of the raising/lowering of plasma in the windward/leeward hemispheres. In the 0400–1200 UT period TEC is enhanced in the windward hemisphere (between −15° and −30° MLAT) for a northward wind, while it is enhanced in the 15° to 30° MLAT region for a southward wind, consistent with the low-altitude meridional wind lifting plasma up/down field lines in the windward/leeward hemispheres. Beginning at around 1200 UT solar ionization again raises TEC levels throughout the low-latitude region. While the northern anomaly crest appears during this time, the southern crest does not appear in any of the LLIONS runs. Both the absence of the southern crest and the comparatively low northern crest TEC levels may be attributed to a weak superfountain. However, the data reveal that the southern crest is practically nonexistent during this time period. The data results from the preceding section suggest that a CPZ suppressed the southern crest during this time.

It is apparent from Fig. 5 that a 50 m/s northward wind injected into a LLIONS run driven by Jicamarca ISR vertical drifts best reproduces the stormtime low-latitude plasma distribution on 9–10 November. As with the data TEC, peak crest TEC values are achieved approximately 2.5 UT hours after the maximum upward drift is achieved at the geomagnetic equator. The local TEC minimum at 2000 UT on 10 November within the northern crest also appears in the model. This feature corresponds to a local minimum in the equatorial drift, offset by a delay of ∼2.5 UT hours. Clearly, the vertical plasma velocity at the geomagnetic equator is the most important factor controlling the latitudinal distribution of plasma.

The 50 m/s northward wind run reproduces another important feature of the data: the faster decay rate of the northern crest relative to the southern. This feature is clearly reflected in model results on 9 November (0000–0600 UT and 2200–2400 UT). However, the decay rate in the 2200–2400 UT period is not quite as rapid as observed in the data, consistent with a northward wind slightly exceeding 50 m/s. It is worth noting that no latitudinal variation in decay rate is seen in the model results on the 10th during the 2200–2400 UT period. Examination of the Jicamarca ISR drifts shows that unlike the periods on the 9th, when the vertical plasma drift at the equator was strongly downward, the drift on the 10th is actually slightly positive between 2000 and 2400 UT. Thus, while the F-peak is still lower in the Northern Hemisphere due to the wind, the ionosphere is not moving downward into regions of high neutral particle concentration, thereby minimizing the differential effect due to faster Northern-Hemisphere recombination.

Despite the good general agreement between the 50 m/s LLIONS run and the data, some significant differences exist. The most obvious difference is that the sudden and sustained suppression of southern crest TEC between 0800 and 2400 UT on 10 November is completely absent in the model results. Indeed, none of the model runs produced this effect, suggesting that winds cannot asymmetrically suppress TEC as deeply and rapidly as was observed on the 10th. These results are consistent with GUVI and other observations that show that this feature was likely caused by a CPZ. Additionally, a latitudinal TEC asymmetry exists between 0400 and 1200 UT on both days that is not present in the data. It appears that during this time, the modeled wind is overestimated, leading to over-suppressed TEC levels north of the geomagnetic equator.

6. Discussion

Observations and model results show that strong stormtime effects penetrated to low latitudes during the November 2004 Superstorm. A strong Eastward penetration electric field penetrated to low latitudes between 1900 and 2100 UT on 9 November, initiating superfountain conditions. Subsequently, maximum Appleton anomaly crest densities were achieved at 2200 UT, with crests displaced as far as ±20° geomagnetic latitude. A strong Westward electric field then caused plasma to drift downward at low latitudes, beginning at ∼2330 UT. The downdrafting plasma, coupled with the onset of sunset, results in the rapid decay of plasma at all latitudes, most noticeably at anomaly crest locations. TEC at crest locations remains stable until approximately 0800 UT on 10 November, when it appears that a CPZ from the southern polar region arrives and suppresses TEC levels by accelerating recombination reactions. Southern crest TEC levels remain suppressed throughout the day on 10 November, even while the northern crest recovers. During both days, it appears that a northward meridional neutral wind causes asymmetries in the TEC distribution, most noticeably during the daytime hours.

It is clear from electric field and TEC observations that the zonal electric field near the geomagnetic equator is the most important driver of low-latitude electrodynamics. The huge TEC fluctuations on the 9th are highly correlated with the electric field – as reflected by the Jicamarca vertical drift velocity – with a lag of approximately 2–2.5 h. Even small perturbations in the zonal field can have significant consequences for crest TEC levels. For example, the decrease in plasma rise velocity between 1500 and 1900 UT on 10 November results in a subsequent local daytime TEC minimum at 2030 UT. Moreover, aside from the action of CPZs or asymmetrical meridional neutral winds, LLIONS reproduces EIA TEC levels and the latitudinal extent of the crests quite well using only accurate JRO drift measurements.

Our results stand in contrast to the results of Lin et al. (2005a), who found (for the October 2003 superstorm) that stormtime wind surges in both hemispheres have a significant impact on crest TEC levels, the height of the F-peak at crest latitudes, and to a lesser extent the maximum latitudinal extent of the crests. Unlike the asymmetric wind effects discussed here, which cause relatively minor adjustments in relative N/S EIA crest TEC levels, Lin et al. found that sustained equatorward winds in both

hemispheres were needed to sustain high TEC levels at the anomaly peaks. The equatorward winds had the effect of lifting the plasma to regions of comparatively low recombination rate at altitudes below 600 km, as well as slowing the descent of superfountain plasma at altitudes above 600 km. In particular, Lin et al. found that simulated crest TEC levels were much lower than observed TEC levels if only vertical $\mathbf{E}\times\mathbf{B}$ drifts were included in the simulation. In our study of the November 2004 superstorm, crest TEC levels are easily created and maintained by driving the LLIONS model with only $\mathbf{E}\times\mathbf{B}$ drifts. The difference between the two studies may be due to the large natural variability seen in many effects between storms. Alternatively, the difference may be an artifact of the models used (i.e., SUPIM driven by TIEGCM neutral densities and winds vs. an ensemble of LLIONS runs with various injected meridional winds).

Another curious discrepancy is apparent in the November 2004 and October 2003 superstorm TEC observations. Following the time of maximum vertical uplift at the geomagnetic equator, the EIA crests extend to $\pm30^\circ$ for the 2003 storm (Lin et al., 2005b), but only $\pm20^\circ$ geomagnetic latitude for the 2004 storm. However, the maximum ROCSAT-derived $\mathbf{E}\times\mathbf{B}$ drifts for the 2003 storm ($\sim$105 m/s at 300 km) are actually smaller than the maximum-observed ISR drifts at comparable altitudes ($>$120 m/s above 100 km for the 2004 superstorm). Since the latitudinal extent of the EIA crests is primarily determined by the vertical drift at the geomagnetic equator, it would appear that the ROCSAT-derived drifts sometimes underestimate the true drift. This would not be surprising given the unavoidable limitations imposed by the satellite platform. Simulations performed by Lin et al. (2005a), however, show that ROCSAT-derived velocity estimates do yield crests at $\pm30^\circ$, suggesting that the ROCSAT drifts are not in error. What could cause the contradiction? While ROCSAT velocities at low altitudes may be underestimated, velocity estimates at higher altitudes are much higher—well over 150 m/s at 2000 km altitude. The greater rise velocity at higher altitudes could cause plasma to drift downward along field lines to higher latitudes, thereby leading to EIA crests extending to $\pm30^\circ$. If ROCSAT low-altitude ($<$400 km) drifts are in fact underestimated, this could explain the results of Lin et al. (2005a), where the TIEGCM model with no winds drives the SUPIM model (CASE 2, their Fig. 5). Specifically, the underestimated low-altitude drifts could be the cause of the low EIA TEC levels, rather than the absence of equatorward neutral winds in both hemispheres, since the quantity of plasma transported out of the equatorial region to higher latitudes is proportional to the vertical drift. Thus, if ROCSAT-derived low-altitude drifts are in error, it may be the case that the 2003 superstorm TEC may be driven almost exclusively by the superfountain effect (not considering CPZ effects), rather than by a combination of the superfountain effect and equatorward stormtime winds.

LLIONS model results indicate that a 50 m/s northward meridional wind exists during much of the period under consideration. In particular, a 50 m/s northward wind replicates the N/S TEC asymmetry seen in the anomaly crests during local time daylight hours (0600–1900 LT on both 9–10 November). During the evening hours, the neutral wind situation is less clear. Between 0700 and 1600 UT (0130 and 1030 LT) on 10 November, southern crest TEC is highly depleted, while northern anomaly TEC remains relatively constant, exactly the reverse of what one would expect from a northward wind. While it is true a southward wind of magnitude 50 m/s could produce such a distribution of plasma, the continued suppression of TEC throughout the following day (1600–2400 UT, 1030–1830 LT), combined with GUVI and GRACE observations, strongly indicate that a CPZ was the cause. Another discrepancy between the model and observed TEC occurs between 0400 and 1200 UT (2230 and 0630 LT) on 9 November. During this time, the latitudinally symmetric TEC distribution seen in Fig. 2 suggests that little, if any meridional wind is present. To summarize, it appears that while a northward 50 m/s exists during daylight hours in the low-latitude region, a much-reduced meridional wind blows during the evening hours. While it is to be expected that some of the inferred 50 m/s northward wind is due to nominal seasonal/diurnal winds, some of it may be the result of differential auroral heating in the two hemispheres. The only way to resolve this issue is through direct measurements and comparison of stormtime winds with nominal seasonal/diurnal winds.

Observations suggest that a CPZ propagated to low latitudes from the southern auroral region, while LSTIDs propagated to low latitudes from northern auroral region. It is true that the GRACE data may be interpreted as a propagating TAD rather than a CPZ (Burke et al., this issue). However, the relatively low propagation velocity ($\sim$230 m/s, compared with $\sim$800 m/s for typical LSTIDs at this altitude), combined with timing coincidental with a reduced $[O/N_2]$ ratio and a TEC decrease at southern low latitudes, leads us to conclude that this was in fact a CPZ blown southward by background and stormtime winds. The propagation of a CPZ to low latitudes in one hemisphere but not the other, as appears the case here, may result from some combination of differential heating in the two auroral regions and/or nominal seasonal and diurnal neutral winds. It is not possible in the present study to determine the role of differential auroral heating. However, the seasonal meridional winds were northward during the November 2004 Superstorm. Thus, the nominal background winds should facilitate the penetration of composition perturbations to low latitudes in the South, but suppress them in the North. Additionally, the seasonal wind would be expected to wind-filter TIDs traveling northward, but to allow TIDs to propagate southward essentially unimpeded. Thus, during solstice geomagnetic storm conditions, the expectation would be to observe CPZs at low latitudes in one hemisphere, and TIDs in the other.

7. Conclusions

The diverse, global observations of the 2004 Superstorm have yielded new information regarding the primary drivers of stormtime low-latitude plasma dynamics. In particular, Jicamarca drift velocity measurements at the geomagnetic equator, combined with the LLIONS model, have made it possible to learn more about the relative contributions of vertical $\mathbf{E}\times\mathbf{B}$ drift and meridional neutral winds in shaping the low-latitude plasma distribution. GUVI and GRACE data have also made it possible to examine the impact of CPZs. It is clear that penetration electric fields, CPZs, and meridional neutral winds all play important roles. The combined observations allow us to draw several conclusions about this storm in particular:

1. Superfountain conditions occurred between $\sim$1900 and 2100 UT on 9 November.
2. The superfountain vertical drifts, the largest ever observed, produced EIA crests extending to $\pm20^\circ$ geomagnetic latitude.
3. Meridional thermospheric neutral winds played a significant role in enhancing daytime EIA TEC levels in the leeward crest, while suppressing TEC in the windward hemisphere.
4. A CPZ rapidly quenched southern EIA crest TEC levels at $\sim$0900 UT on 10 November. TEC levels remained suppressed for the next 16+ h.

In addition to these specific conclusions, it is possible to draw some general conclusions about low-latitude stormtime effects. First, it is clear that low-latitude TEC is highly responsive to perturbations in the zonal electric field that are either of large

amplitude and short duration (e.g., ~1900–2100 UT on 9 November) or small amplitude and long duration (e.g., ~1600–2000 UT on 10 November). The effects of such perturbations are typically seen in the low-latitude TEC distribution, with a time lag of between ~2 and 2.5 h. Conversely, perturbations that are both small amplitude and small duration have minimal impact on low-latitude TEC. Second, it appears that superfountain conditions alone are, at least under certain storm conditions, sufficient to produce widely separated EIA crests with high TEC levels. Whereas the SUPIM model, driven by TIEGCM, suggests that equatorward thermospheric winds are needed to create and sustain widely separated, high-TEC EIA crests, the LLIONS model results in this report suggest otherwise. We suggest that the cause for this discrepancy could be an underestimation of the ROCSAT-derived vertical drifts used to drive the SUPIM/TIEGCM model. Third, it appears that meridional neutral winds can act to accelerate the nighttime decay of the leeward EIA crest, while sustaining TEC levels in the windward crest. This effect is believed to be the result of lowering and raising the leeward and windward F-layers, respectively.

The large spatial scales involved, as well as the complexity of the plasma dynamics, make it clear that satellite observations, combined with ground-based distributed observatories, are an effective way to study superstorms. However, much work needs to be done if future superstorms are to be studied in as much detail as the November 2004 superstorm. Most importantly, this work has shown that accurate measurements of vertical equatorial plasma velocity are needed. It was primarily by fortuitous coincidence that the Jicamarca ISR was switched on and in the appropriate mode to take these measurements. Magnetometer measurements (Anderson et al., 2002, 2004a) have been shown to be an effective means of determining the daytime $\mathbf{E} \times \mathbf{B}$ drifts, while ionosondes have been shown to be modestly effective at measuring nighttime drifts when convection effects dominate (Anderson et al., 2004b). Together, these two techniques may provide a more reliable alternative to ISR measurements. Almost as crucial to future studies is the addition of accurate measurements of the meridional thermospheric wind. Such measurements will be needed to ascertain the role of winds on the equatorward propagation of CPZs and LSTIDs. Additionally, measurements of meridional neutral winds would help determine the relative role of differential heating in causing CPZs and/or LSTIDs to be triggered in one hemisphere but not the other. Finally, wind measurements could help determine the importance of winds in creating and maintaining high EIA crest TEC levels.

Acknowledgements

This work was supported by the National Science Foundation (NSF grant #0521487). The work at Boston College was partially supported by the Air Force Research Laboratory through AFOSR task 2311AS. The authors wish to express their gratitude to Dr. Vince Eccles of the Space Environment Corporation for making the LLIONS model available. The authors are also grateful to the TIMED/GUVI and GRACE teams for making available their data sets.

References

Anderson, D., Anghel, A., Yumoto, K., Ishitsuka, M., Kudeki, E., 2002. Estimating daytime vertical E × B drift velocities in the equatorial F-region using ground-based magnetometer observations. Geophys. Res. Lett. 29, 37-1.

Anderson, D., Anghel, A., Chau, J., Veliz, O., 2004a. Daytime vertical E × B drift velocities inferred from ground-based magnetometer observations at low latitudes. Space Weather 2, 11001.

Anderson, D., Anghel, A., Araujo, E., Eccles, V., Valladares, C., Lin, C., 2006. Theoretically modeling the low-latitude, ionospheric response to large geomagnetic storms. Radio Sci. 41, RS5S04.

Anderson, D.N., 1973. A theoretical study of the ionospheric F region equatorial anomaly-I. Theory. Planet. Space Sci. 21, 409–419.

Anderson, D.N., 1981. Modeling the ambient, low latitude F-region ionosphere—a review. J. Atmos. Terr. Phys. 43, 753–762.

Anderson, D.N., Reinisch, B., Valladare, C., Chau, J., Veliz, O., 2004b. Forecasting the occurrence of ionospheric scintillation activity in the equatorial ionosphere on a day-to-day basis. J. Atmos. Sol. Terr. Phys. 66, 1567–1572.

Blanc, M., Richmond, A.D., 1980. The ionospheric disturbance dynamo. J. Geophys. Res. 85, 1669–1686.

Bruinsma, S., Tamagnan, D., Biancale, R., 2004. Atmospheric densities derived from CHAMP/STAR accelerometer observations. Planet. Space Sci. 52, 297–312.

Bruinsma, S., Biancale, R., 2003. Total densities derived from accelerometer data. J. Spacecr. Rockets 40, 230–236.

Burke, W.J., et al. J. Atmos. Sol. Terr. Phys., this issue.

Eccles, J.V., Anderson, D., Anghel, A., Valladares, C., Sojka, J.J., 2004. Assessing a low-latitude ionosphere model driven with data-determined E × B drifts. American Geophysical Union, Spring Meeting 2004, abstract #SA42A-02.

Erickson, P.J., Goncharenko, L.P., 2009. Dynamics of North American sector ionospheric and thermospheric response during the November 2004 superstrom. J. Atmos. Sol. Terr. Phys., this issue, doi:10.1016/j.jastp.2009.04.001.

Fejer, B.G., Gonzales, C.A., Farley, D.T., Kelley, M.C., Woodman, R.F., 1979. Equatorial electric fields during magnetically disturbed conditions. 1. The effect of the interplanetary magnetic field. J. Geophys. Res. 84, 5797–5802.

Fejer, B.G., Spiro, R.W., Wolf, R.A., Foster, J.C., 1990. Latitudinal variation of perturbation electric fields during magnetically disturbed periods—1986 Sundial observations and model results. Ann. Geophys. 8, 441–454.

Fejer, B.G., Scherliess, L., 1995. Time dependent response of equatorial ionospheric electric fields to magnetospheric disturbances. Geophys. Res. Lett. 22, 851–854.

Hargreaves, J.K., 1992. The Solar-Terrestrial Environment. Cambridge University Press, Cambridge.

Kelley, M.C., Fejer, B.G., Gonzales, C.A., 1979. An explanation for anomalous equatorial ionospheric electric fields associated with a northward turning of the interplanetary magnetic field. Geophys. Res. Lett. 6, 301–304.

Kelley, M.C., 1989. The Earth's Ionosphere: Plasma Physics and Electrodynamics. Academic Press, San Diego.

Kelley, M.C., et al., 2009. Spectacular low- and mid-latitude electrical fields and neutral winds during a superstorm. J. Atmos. Sol. Terr. Phys., this issue, doi:10.1016/j.jastp.2008.12.006.

Kudeki, E., Bhattacharyya, S., Woodman, R.F., 1999. A new approach in incoherent scatter region E/times B drift measurements at Jicamarca. J. Geophys. Res. 104, 28145.

Lin, C.H., et al., 2005a. Theoretical study of the low- and midlatitude ionospheric electron density enhancement during the October 2003 superstorm: relative importance of the neutral wind and the electric field. J. Geophys. Res. 110, 12312.

Lin, C.H., et al., 2005b. Large-scale variations of the low-latitude ionosphere during the October–November 2003 superstorm: observational results. J. Geophys. Res. 110.

Richmond, A.D., Peymirat, C., Roble, R.G., 2003. Long-lasting disturbances in the equatorial ionospheric electric field simulated with a coupled magnetosphere–ionosphere–thermosphere model. J. Geophys. Res. 108, 1118.

Rishbeth, H., et al., 2000. Annual and semiannual variations in the ionospheric F2-layer: II. Physical discussion. Ann. Geophys. 18, 945–956.

Scherliess, L., Fejer, B.G., 1999. Radar and satellite global equatorial F region vertical drift model. J. Geophys. Res. 104, 6829–6842.

Schunk, R.W., Sojka, J.J., 1997. Global ionosphere-polar wind system during changing magnetic activity. J. Geophys. Res. 102, 11625–11652.

Strickland, D.J., Evans, J.S., Paxton, L.J., 1995. Satellite remote sensing of thermospheric O/N_2 and solar EUV. 1: Theory. J. Geophys. Res. 100, 12217.

Strickland, D.J., et al., 2004. Quiet-time seasonal behavior of the thermosphere seen in the far ultraviolet dayglow. J. Geophys. Res. 109, 01302.

Tsurutani, B.T., et al., 2007. Oxygen ion uplift and satellite drag effects during the 30 October 2003 daytime superfountain event. Ann. Geophys. 25, 569–574.

Valladares, C.E., Sheehan, R.E., 2001. Measurement of the latitudinal distributions of total electron content during equatorial spread F events. J. Geophys. Res. 106, 29133–29152.

Valladares, C.E., Sheehan, R., Villalobos, J., 2004. A latitudinal network of GPS receivers dedicated to studies of equatorial spread F. Radio Sci. 39, RS1S23.

Zhang, Y., et al., 2004. O/N_2 changes during 1–4 October 2002 storms: IMAGE SI-13 and TIMED/GUVI observations. J. Geophys. Res. 109, 10308.